PAPER • **OPEN ACCESS**

Thermal Performance Analysis in Sinusoidal-Cavities-Ribs Microchannel Heat Sink with Secondary Channel Geometry for Low Pumping Power Application

To cite this article: W M A A Japar *et al* 2020 *IOP Conf. Ser.: Mater. Sci. Eng.* **884** 012087

Thermal Performance Analysis in Sinusoidal-Cavities-Ribs Microchannel Heat Sink with Secondary Channel Geometry for Low Pumping Power Application

W M A A Japar[1,4], N A C Sidik[1], R. Saidur[2], Y Asako[1] and N M Muhammad[3]
[1] Malaysia-Japan International Institute of Technology, Universiti Teknologi Malaysia, Kuala Lumpur, MALAYSIA
[2] Research Centre for Nano-Materials and Energy Technology, School of Science and Technology, Sunway University, Bandar Sunway, 47500 Subang Jaya, Selangor, MALAYSIA
[3] Faculty of Engineering, Kano University of Science and Technology, Wudil, NIGERIA

E-mail: arifklang@gmail.com, azwadi@utm.my, y.asako@utm.my, saidur@sunway.edu.my and nuramuaz@gmail.com

Abstract. The increases in the demand for high performance electronic device has led cooling technology from air cooling to liquid cooling method in order to prevent the operating temperature in the electronic device goes beyond the junction temperature of the electronic device. Liquid as a heat transportation in a micro-cooling technology is an effective method to maintain the operating temperature. Among the micro-cooling technology, microchannel heat sink appears as a promising method that provides high heat transfer rate with minimal pressure drop. However, the conventional microchannel heat sink which has straight channels (CR MCHS) inadequate to remove high heat flux generated by the current devices due to high thermal resistance in laminar region. High heat transfer rate just can be obtained in the microchannel heat sink by using a large mass flowrate which affects the pumping power consumption. The method is not suitable for the low pumping power application. So instead of increases the mass flowrate, in this paper, a hybrid microchannel heat sink was proposed in order to satisfy the cooling demand with low pumping power consumption. The effect of sinusoidal cavities, rectangular ribs and secondary channel geometry on thermal resistance and pumping power in the hybrid microchannel sink (SD-RR-SC MCHS) was studied numerically. The result showed the SD-RR-SC MCHS and RR MCHS had the lowest thermal resistance and temperature variation for the mass flowrate that less than 6.78×10^{-5} kg/s. Despite both designs had a similar thermal performance with the average deviation of 5%, SD-RR-SC MCHS required only 11.3% of CR MCHS pumping power, while RR MCHS required 31.3% of CR MCHS pumping power in order to achieve the optimum thermal performance of CR MCHS. Means, SD-RR-SC MCHS is the most suitable design which can fulfil cooling demand for low pumping power application.

[4] arifklang@gmail.com

1. Introduction

Fast development in electronic industry has witnessed many intelligent electronic devices which carry high power density in its microchips. As the power density increases with the number of transistor in the microchips, high heat flux is generated by the electronic device and thus increases the operating temperature of the electronic device. In order to prevent the operating temperature goes beyond the junction temperature, the electronic device reduces the system performance so as can reduce the operating temperature. Nowadays, thermal management is very important to maintain the operating temperature below than junction temperature. The junction temperature for semiconductor [1] or electronic device [2] should less than 358.15 K. In order to fulfill the cooling demand, intensive study about the microchannel heat sink performance has been conducted by many researchers due to remarkable heat transfer characteristic, smaller size and less noisy.

The concept of microchannel heat sink was established by Tuckerman and Pease in 1981 [3]. They revealed that, microchannel heat sink can remove heat flux up to 100W/cm^2. However, in the recent year, the shrinking size of electronic devices has been increasing the power density at an unpredicted rate [4, 5]. As a consequence, the conventional design that was proposed by Tuckerman and Pease [3] which is the straight channel microchannel heat sink inadequate to remove the such heat flux generated by current device. Therefore, the enhanced microchannel heat sink with a great extent of heat removal capability has been being developed by many inventors. Generally, the heat removal capability of microchannel heat sink can be improved by active or passive method. Passive method becomes the most used technique among researchers due to no moving part and no external energy will be involved in the heat transfer improvement [6]. In term of economic management, thermal enhancement with minimal pumping power becomes as a direction in design development of enhanced microchannel heat sink for many researchers.

In order to achieve the high heat transfer performance with minimal pressure drop, combined effect of passive method in hybrid microchannel heat sink has been proposed by some researchers in open literature. Gong and his teammate [7] was studied the combined effect of dimple and wavy channel. They found that, by having convex dimple geometry in the wavy channel, remarkable heat transfer enhancement with significant reduction of flow resistance was obtained. In 2016, Li and his co-researchers [8] investigated the effect of ribs and triangular cavities geometry combination (TC-RR MCHS) on fluid flow and heat transfer characteristic. They demonstrated that, flow disruption at the central of microchannel heat sink provided by rectangular ribs increased the flow mixing and thus improved the heat transfer performance. Besides that, the triangular cavities also increased the heat transfer performance by providing larger heat transfer area. After that, Japar and his co-researchers [9] tried to study the effect of the triangular cavities geometry shape on TC-RR MCHS performance. However, the design has a problem with vortices dead zone at the triangular cavities corner. Due to this problem, Japar et al., [10, 11] has proposed secondary channel geometries that connect two adjacent main channels. The channel was connected through triangular cavities. They illustrated that secondary flow from adjacent channel eliminated the vortices dead zone in the triangular cavities. The mechanism helped to prevent concentration heat flux in the cavities area.

All of the previous studies show that high heat transfer rate with minimal pressure drop can be obtained at high Re number which affect the pumping power consumption. However, to the best of author's knowledge, there has no researcher that study about the optimum overall performance enhancement at low Re number which contributes to reduction of pumping power consumption. In this paper, deep analysis on our previous work [12, 13] are conducted by analysing the effect of sinusoidal cavities, rectangular ribs and secondary channels geometry on thermal resistance, temperature variation and pumping power. Comparative analysis between sinusoidal cavities with rectangular rib and secondary channel microchannel heat sink (SD-RR-SC MCHS) with related geometries such as conventional rectangular microchannel heat sink (CR MCHS), rectangular rib microchannel heat sink (RR MCHS), sinusoidal cavities microchannel heat sink (SD MCHS) and sinusoidal cavities with rectangular rib microchannel heat sink (SD-RR MCHS) is conducted in order to highlight the strength of SD-RR-SC MCHS.

2. Geometry Parameter of Microchannel Heat Sink

This microchannel heat sink is made by copper and consist of ten microchannels. However, in order to save the computational cost, only one symmetrical part of the microchannel heat sink is adopted in present simulation as shown in Figure 1(a). Table 1 shows parameter valued for the geometry that illustrated in Figure 1(b). In order to study the effectiveness of secondary flow on hybrid microchannel heat sink performance, design development is started from reference design (CR MCHS) to single passive technique design (RR MCHS and SD MCHS). Next, hybrid design (SD-RR and SD-RR-SC) is developed based on the strength and weakness that found in single passive technique designs.

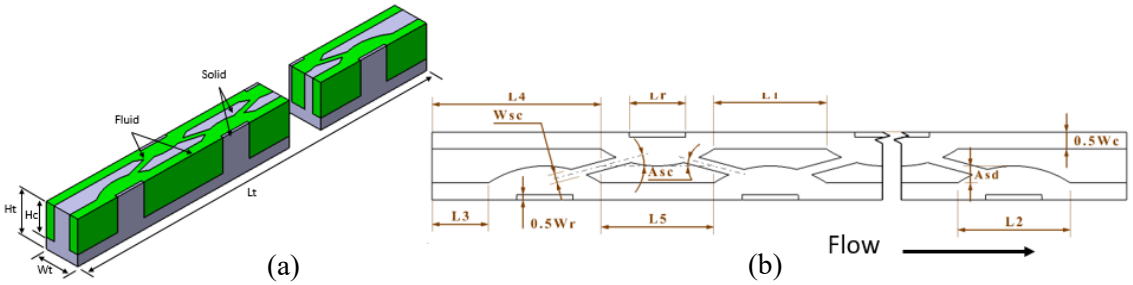

Figure 1. SD-RR-SC MCHS (a) One symmetrical part (b) Geometry parameter.

Table 1. Geometry parameters of SD-RR-SC MCHS.

Lt (µm)	Wt & Hc (µm)	Ht (µm)	Wc (µm)	Lr & L3 (µm)	Wr (µm)	L1, L2 & L5 (µm)	L4 (µm)	Wsc (µm)	Asc (°)	Asd (µm)
10000	300	400	150	250	45	500	750	40	15	75

3. Numerical Analysis Approach

The three dimensional fluid flow and heat transfer equations are solved by ANSYS 17.0 software. The fluid flow in all enhanced microchannel heat sinks are assumed as continuum due to Knudsen number of the fluid flow is less than (10^{-3}) [14]. Means, Navier-Stokes equation and non-slip boundary condition are applicable in this analysis. The fluid in those enhanced microchannel heat sinks are assumed as Newtonian, incompressible and constant thermophysical properties. The other assumption that made in this analysis are: (a) The flow is laminar (b) Steady-state condition (c) Gravitational force viscous dissipation and radiation heat transfer are neglected.

3.1. Governing Equations

Governing equations for continuity, momentum and energy equations are written as equation (1), equation (2) – (4) and equation (5) – (6), respectively, after considering the assumption that made in this study.

$$\frac{\partial u}{\partial x}+\frac{\partial v}{\partial y}+\frac{\partial w}{\partial z}=0 \tag{1}$$

$$u\frac{\partial u}{\partial x}+v\frac{\partial u}{\partial y}+w\frac{\partial u}{\partial z}=-\frac{1}{\rho_f}\frac{\partial p}{\partial x}+\frac{\mu_f}{\rho_f}\left(\frac{\partial^2 u}{\partial x^2}+\frac{\partial^2 u}{\partial y^2}+\frac{\partial^2 u}{\partial z^2}\right) \tag{2}$$

$$u\frac{\partial v}{\partial x}+v\frac{\partial v}{\partial y}+w\frac{\partial v}{\partial z}=-\frac{1}{\rho_f}\frac{\partial p}{\partial y}+\frac{\mu_f}{\rho_f}\left(\frac{\partial^2 v}{\partial x^2}+\frac{\partial^2 v}{\partial y^2}+\frac{\partial^2 v}{\partial z^2}\right) \tag{3}$$

$$u\frac{\partial w}{\partial x}+v\frac{\partial w}{\partial y}+w\frac{\partial w}{\partial z}=-\frac{1}{\rho_f}\frac{\partial p}{\partial z}+\frac{\mu_f}{\rho_f}\left(\frac{\partial^2 w}{\partial x^2}+\frac{\partial^2 w}{\partial y^2}+\frac{\partial^2 w}{\partial z^2}\right) \tag{4}$$

$$u\frac{\partial T_f}{\partial x}+v\frac{\partial T_f}{\partial y}+w\frac{\partial T_f}{\partial z}=\frac{k_f}{\rho_f c_{Pf}}\left(\frac{\partial^2 T_f}{\partial x^2}+\frac{\partial^2 T_f}{\partial y^2}+\frac{\partial^2 T_f}{\partial z^2}\right) \quad (5)$$

$$0=k_s\left(\frac{\partial^2 T_s}{\partial x^2}+\frac{\partial^2 T_s}{\partial y^2}+\frac{\partial^2 T_s}{\partial z^2}\right) \quad (6)$$

Where the velocity component in *x, y* and *z*-directions are denoted as *u, v and w*, respectively. While fluid density, fluid viscosity, fluid pressure, fluid temperature, fluid thermal conductivity and fluid specific heat are denoted as ρ_f, μ_f, p, T_f, k_f and Cp_f, respectively. For solid region, temperature and thermal conductivity are denoted as T_s and k_s, respectively.

3.2. Boundary Condition

Boundary condition is a condition for hydrodynamic and thermal that we applied on the simulated geometries in the present study. Table 2 shows the details for the boundary conditions.

Table 2. Boundary condition.

Boundary	Location	Condition
Hydrodynamic	At the fluid-solid interface	No-slip and no penetration $u=v=w=0$ $-k_s\left(\frac{\partial T_s}{\partial n}\right)=-k_f\left(\frac{\partial T_f}{\partial n}\right)$ where n is the coordinate normal to the wall
	At inlet, $x=0$	$u_f=u_{in}$ (uniform velocity) $v=w=0$
	At outlet, $x=L_t=10mm$	$p_f=p_{out}=1atm$
Thermal	At inlet, $x=0$	$T_f=T_{in}=300K$ (for water) $-k_s\left(\frac{\partial T_s}{\partial x}\right)=0$ (for solid)
	At outlet, $x=L_t=10mm$	$-k_f\left(\frac{\partial T_f}{\partial x}\right)=0$ (for water) $-k_s\left(\frac{\partial T_s}{\partial x}\right)=0$ (for solid)
	At top wall, $z=Ht=0.4mm$	$u=v=w=0$; $-k_s\left(\frac{\partial T_s}{\partial z}\right)=0$
	At bottom wall, $z=0$	$-k_s\left(\frac{\partial T_s}{\partial z}\right)=q=100W/cm^2$
	At side wall, $y=0$	$\frac{\partial}{\partial y}=0$ (symmetry)
	At side wall, $y=Wt=0.3mm$	$\frac{\partial}{\partial y}=0$ (symmetry)

3.3. Verification and Grid Independence Test

In this paper, the hexahedral mapped structure in all simulated microchannel heat sinks are generated by ANSYS ICEM (as shown in Figure 2). Finite volume method is used to discretize the governing equation in the hexahedral mapped structure. The SIMPLE algorithm is employed in all simulation analyses in order to accomplish the pressure-velocity coupling. Besides that, second order upwind and second order central difference scheme are utilized for the convective and diffusion term, respectively.

In order to control the accuracy and stability of simulation result, the convergence criteria for continuity and energy are set to 10^{-6} and 10^{-9}, respectively.

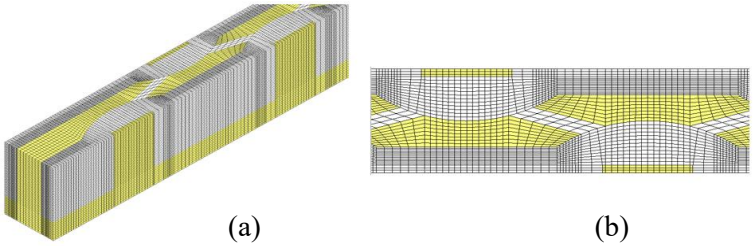

(a) (b)

Figure 2. Computational grid of SD-RR-SC MCHS (a) Isometric view (b) Top view at x-z plane

Verification of a numerical model is very important to ensure the used approach in this study is correct and can be implemented to the enhanced microchannel heat sink analysis. For verification purpose, the straight channel MCHS (CR MCHS) with the element number of 1.5 million (finest grid) was used in order to verify the Local Nu number and pressure drop in the MCHS with the correlations provided by Philips [15] and Steinke & Kandlikar [16], respectively. The correlations can be written as below:

$$Nu_X = 1.0958\left[\frac{23.315+27038(X)+1783300(X)^2}{1+3049(X)+472520(X)^2-35714(X)^3}\right] \tag{7}$$

$$X = \frac{x}{D_h \,\mathrm{Re}\,\mathrm{Pr}} \tag{8}$$

$$\Delta p = \frac{2(f\,\mathrm{Re})\mu_f u_m Lt}{D_h^2} + \frac{K\rho_f u_m^2}{2} \tag{9}$$

$$f\,\mathrm{Re} = 24\left(1-1.3553\alpha_c+1.9467\alpha_c^2+1.7012\alpha_c^3+0.9564\alpha_c^4+0.2537\alpha_c^5\right) \tag{10}$$

$$K = 0.6797+1.2197\alpha_c+3.3089\alpha_c^2-9.5921\alpha_c^3+8.9089\alpha_c^4-2.9959\alpha_c^5 \tag{11}$$

Where α_c and K are channel aspect ratio of width to height and Hagenbach's factor, respectively. Verification of the simulation approach with the correlations are illustrated in Figure 3. It clearly shows the simulation results have a good agreement with the both correlations. This agreement indicates that the simulation approach can be implemented in further analysis order to predict the fluid flow and heat transfer characteristic in enhanced MCHS.

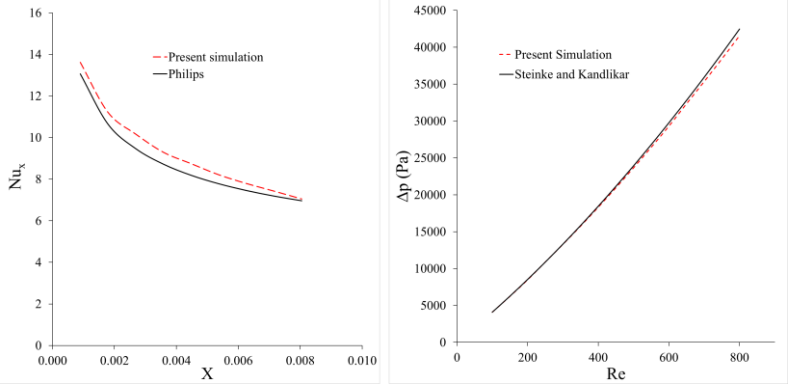

Figure 3. Model validation (a) Local Nusselt number according to Philips [15] (b) Pressure drop according to Steinke & Kandlikar [16].

In order to find the optimum number of element and check the grid sensitivity, the grid independency test was conducted for the CR MCHS. The test was started with the finest grid (1.5 million) and reduced to coarser grid (0.7 million) as shown in Table 3. The average Nu number and pressure drop are taken as a reference parameter for the test. The test shows that, the element number of 1.3 million has a reasonable accuracy compared to other coarser grids. Means that, the element number of 1.3 million can be adopted to the other designs in this study.

Table 3. Grid independence test

Grid number ($X10^6$)	Nu	*e%*	Pressure drop (Pa)	*e%*
1.5	10.23	-	41572.54	-
1.3	10.24	0.10	41524.38	0.12
1.1	10.24	0.10	41482.03	0.22
0.9	10.25	0.20	41394.09	0.43
0.7	10.26	0.29	41189.63	0.92

4. Data Processing

This section presents the relevant expressions that used to calculate the characteristics of heat transfer and fluid flow in MCHS. Re number, hydraulic diameter and apparent friction factor are expressed in equation (12), equation (13) and equation (14), respectively.

$$\mathrm{Re} = \frac{\rho u_m D_h}{\mu} \tag{12}$$

$$D_h = \frac{2H_c W_c}{H_c + W_c} \tag{13}$$

$$f_{app,ave} = \frac{2D_h \Delta P}{Lt\rho u_m^2} \tag{14}$$

Where D_h, L_t and ΔP are hydraulic diameter, total length of microchannel and pressure drop across microchannel, respectively. Average heat transfer coefficient and the average Nusselt number are given by:

$$h_{ave} = \frac{q_w A_{film}}{A_{con.}(T_{W,ave} - T_{f,ave})} \tag{15}$$

$$Nu_{ave} = \frac{h_{ave} D_h}{k_f} \tag{16}$$

Where q_w, A_{film}, A_{cond}, $T_{w,ave}$ *and* $T_{f,ave}$ are the heat flux per unit area, heated area, convection heat transfer area, average temperature of wall and average temperature of fluid, respectively.

In order to investigate the thermal performance of the proposed microchannel heat sink (SD-RR-SC MCHS), thermal resistance, R and temperature variation, T are measured by equation (17) and equation (18), respectively.

$$R = \frac{T_{\max} - T_{\min}}{q_w A_{film}} \tag{17}$$

$$T = T_{\max} - T_{\min} \tag{18}$$

Where $T_{\max}$ and $T_{\min}$ are the maximum temperature and minimum temperature in a microchannel heat sink. Pumping power for each designs is calculated by equation (19).

$$P = \dot{V}\Delta P \tag{19}$$

5. Result and Discussion

Figure 4 shows the thermal resistance, R and temperature variation, T of all microchannel heat sinks. Both graphs illustrate that, thermal resistance, R and temperature variation, T decrease when the mass flowrate in all designs increase. It can be seen that, the highest thermal resistance, R and temperature variation, T were obtained by CR MCHS followed by SD MCHS. Although in the previous work [12] showed the both designs had a similar pattern of streamline distribution profile, the SD MCHS obtains a better thermal performance due to the larger heat transfer area that provided by cavities geometry in SD MCHS. Hybrid microchannel heat sinks such as SD-RR MCHS and SD-RR-SC MCHS exhibit the similar thermal resistance, R and temperature variation, T as thermal microchannel heat sink (RR MCHS) which lower than CR MCHS and SD MCHS. RR MCHS is called as thermal microchannel heat sink attributed to its ability to remove heat flux efficiently compared to other designs. However, in term of economic management, RR MCHS is not the best design compared to SD-RR MCHS and SD-RR-SC MCHS. As we can see in Figure 4, for the mass flowrate that less than $6.78X10^{-5}$ kgs^{-1}, the SD-RR-SC MCHS shows the most similar thermal resistance, R and temperature variation, T as RR MCHS the average deviation of 5%.

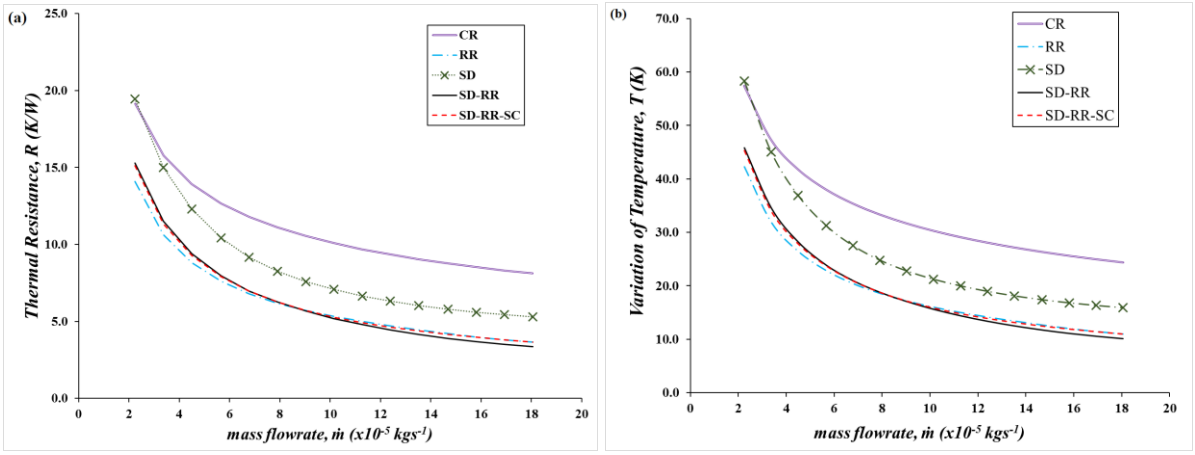

Figure 4. Thermal performance in all microchannel heat sinks (a) Thermal resistance, R (b) Temperature variation, T .

As illustrates in Figure 5, despite RR MCSH exhibits the lower thermal resistance, R and temperature variation, T than SD-RR-SC MCHS, RR MCHS required the higher pumping power, P consumption than SD-RR-SC MCHS due to blocking effect provided by rectangular ribs at the small area in RR MCHS. In SD-RR-SC MCHS, Sinusoidal cavities and secondary channel geometry has minimized the blocking effect by providing the larger flow area at the rectangular ribs area. By comparing the both designs (RR MCHS and SD-RR-SC MCHS) with conventional microchannel heat sink (CR MCHS), CR MCHS required 18 kgs^{-1} to achieve the lowest thermal resistance, R (8.1 K/W) and temperature variation, T (24.3 K) for its design with the pumping power, P of 7.52 mW, while SD-RR-SC only required 11.3% of CR MCHS pumping power, P in order to achieve the lowest thermal resistance, R and temperature variation, T of CR MCHS. However, due to the blocking effect in the small area, RR MCHS required little bit higher pumping power, P than SD-RR-SC MCHS, 31.3% of CR MCHS pumping power, P. From the view of economic management, SD-RR-SC MCHS is the best design which can provide remarkable heat transfer performance as thermal microchannel heat sink (RR MCHS) with low pumping power consumption.

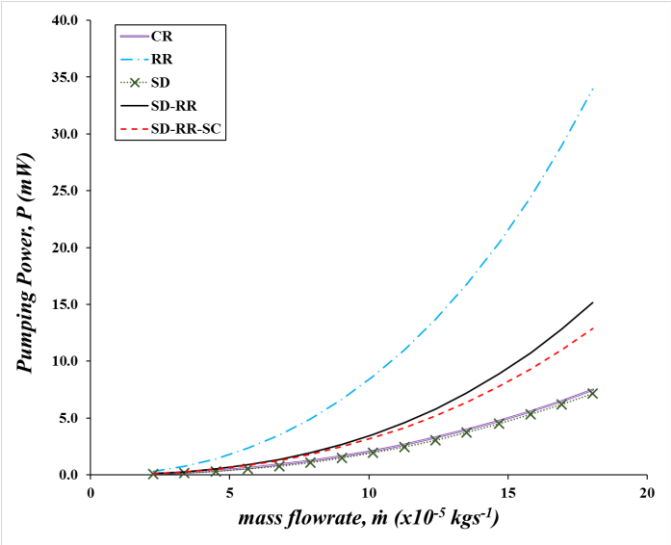

Figure 5. Pumping power consumption of all microchannel heat sinks.

6. Conclusion

In this study, the combined effect of sinusoidal cavities, rectangular ribs and secondary channel geometry on thermal resistance, temperature variation and pumping power have been study numerically. This analysis proved that secondary channel geometry feature can help to increase the flow mixing which contributed to the reduction of thermal resistance and temperature variation. Besides that, the feature also helps to reduce pumping power consumption by providing the larger flow area.

Acknowledgment

Authors wish to thanks Universiti Teknologi Malaysia for supporting this research activity under Takasago grant (R.K130000.7343.4B365).

References

[1] Yan Y, Yan H, Yin S, Zhang L and Li L 2019 Single/multi-objective optimizations on hydraulic and thermal management in micro-channel heat sink with bionic Y-shaped fractal network by genetic algorithm coupled with numerical simulation *International Journal of Heat and Mass Transfer* **129** 468-79.

[2] Naqiuddin N H, Saw L H, Yew M C, Yusof F, Poon H M, Cai Z and Thiam H S 2018 Numerical investigation for optimizing segmented micro-channel heat sink by Taguchi-Grey method *Applied Energy* **222** 437-50.

[3] Tuckerman D B and Pease R F W 1981 High-performance heat sinking for VLSI *IEEE Electron device letters* **2** 126-9.

[4] Yan Y, Feng S, Huang Z, Zhang L, Pan W, Li L and Yang Z 2018 Thermal management and catalytic combustion stability characteristics of premixed methane/air in heat recirculation meso-combustors *International Journal of Energy Research* **42** 999-1012.

[5] Yan Y, Yan H, Zhang L, Li L, Zhu J and Zhang Z 2018 Numerical investigation on combustion characteristics of methane/air in a micro-combustor with a regular triangular pyramid bluff body *International Journal of Hydrogen Energy* **43** 7581-90.

[6] Japar W M A A, Sidik N A C, Aid S R, Asako Y and Ken T L 2018 A Comprehensive Review on Numerical and Experimental Study of Nanofluid Performance in Microchannel Heatsink (MCHS) *Journal of Advanced Research in Fluid Mechanics and Thermal Sciences* **45** 165 – 76.

[7] Gong L and Wei B, editors. The Characteristics of Fluid Flow and Heat Transfer in Wavy, Dimple and Wavy-Dimple Microchannels. Applied Mechanics and Materials; 2013: Trans Tech Publ.

[8] Li Y, Xia G, Ma D, Jia Y and Wang J 2016 Characteristics of laminar flow and heat transfer in microchannel heat sink with triangular cavities and rectangular ribs *International Journal of Heat and Mass Transfer* **98** 17-28.

[9] Japar W M A A, Sidik N A C, Saidur R, Asako Y and Mohd M I Temperature Minimization on the Substrate of a Heat Sink By Rib-Groove Microchannel Heat Sink with Effective Energy Consumption: Groove Geometry Parameter Effects.

[10] Japar W M A A, Sidik N A C and Mat S 2018 A comprehensive study on heat transfer enhancement in microchannel heat sink with secondary channel *International Communications in Heat and Mass Transfer* **99** 62-81.

[11] Wan Mohd. Arif Aziz Japar N A C S, M'hamed Beriache 2019 Hydrothermal Performance in a New Designed Hybrid Microchannel Heat Sink with Optimum Secondary Channel Geometry Parameter: Numerical and Experimental Studies *Journal of Advanced Research Design* **54** 13-27.

[12] Japar W and Sidik N A C, editors. The effectiveness of secondary channel on the performance of hybrid microchannel heat sink at low pumping power. Materials Science and Engineering; 2019 2019: IOP Publishing.

[13] Japar W M A A, Sidik N A C and Asako Y Entropy Generation Minimization In Sinusoidal Cavities-Ribs Microchannel Heat Sink Via Secondary Channel Geometry *CFD Letters* **11** 1-10.
[14] Service R F 1998 Coming soon: the pocket DNA sequencer *Science (New York, NY)* **282** 399.
[15] Phillips R J 1990 Microchannel heat sink *Advances in thermal modeling of electronic components and systems* **2** 109-84.
[16] Steinke M E and Kandlikar S G 2006 Single-phase liquid friction factors in microchannels *International Journal of Thermal Sciences* **11** 1073-83.